Eur. Phys. J. B **5**, 223–229 (1998)

THE EUROPEAN PHYSICAL JOURNAL B

Nonlinear dynamics of density waves in granular flows through narrow vertical channels

A. Valance[a] and T. Le Pennec

Groupe Matière Condensée et Matériaux[b], Université Rennes 1, 35042 Rennes Cedex, France

Received: 11 March 1998 / Revised and Accepted: 3 July 1998

Abstract. We study granular flows through narrow channels driven by gravity in the framework of the kinetic theory for dissipative dense gases. We derive equations of motion for quasi-one-dimensional systems. In a certain range of flow density, the steady homogeneous regime is found to be unstable against the formation of density waves. We show moreover that near the onset of the instability, the governing equation for the flow density is a mixture of the Korteweg-de-Vries equation, which leads to soliton, and the Bürger equation which exhibits spatio-temporal chaos. The competition between chaos and solitons may lead either to regular spatially ordered density waves or to chaotic dynamics. We argue that these two types of dynamics can be encountered experimentally according to the channel width and the dissipative properties of the granular media.

PACS. 81.05.rm Porous materials; granular materials – 47.50.+d Non-Newtonian fluid flows – 05.20.Dd Kinetic theory

1 Introduction

The flow of granular media [1,2] gives rise to a variety of dynamical phenomena as wide as, and perhaps even wider, than does the fluid flow. Whereas we have the Navier-Stokes equation as a reliable model for almost all the types of fluid flows, the situation is not so clear in the realm of granular flows where a general and reliable description is not yet available. Nowadays, the only sound theoretical basis for the description of rapid granular flow is the model of Jenkins and Savage [3] which is inspired by the kinetic theory of dense gases. In this paper, we show that the continuum model of Jenkins and Savage can account for the formation of density waves in granular flows through narrow vertical channels. Formation of density waves in such flows has been clearly observed in experiments [4,5] and confirm by numerical simulations [5–7]. The density waves propagate at a slower speed than the mean flow of particles and exhibit frequently a spatial ordering along the flow with a well-defined wavelength [9]. This latter observation supports the idea that the formation of density waves results in a dynamical instability connected to grain inelasticity, as in other granular contexts such as the clustering instability in dissipative gases [8] or the heap formation under vibration [10,11].

Our aim here is to show than the density waves can be explained as the consequence of a dynamical instability. For that purpose, we derive from the model of Jenkins and Savage equations of motion for quasi-one-dimensional flows. We show that the steady homogeneous flow is susceptible to be unstable against small fluctuations. Indeed, we find that below a critical value of the flow density, the steady homogeneous flow destabilizes and gives rise to density waves. Close to the onset of the instability, we extract scaling laws for the wavelength of the most dangerous density fluctuation – which is expected to prevail in the subsequent nonlinear evolution and therefore to govern the density waves dynamics – and for its propagation velocity as a function of the relevant parameters (*i.e.*, the channel width, the roughness of the channel walls and the grain inelasticity). Furthermore a nonlinear analysis reveals that in the vicinity of the instability the governing equation for the flow density is a combination between the Korteweg-De-Vries equation, which leads to soliton, and the Bürger equation, which is known for chaotic behaviour. The competition between chaos and solitons may lead either to regular spatially ordered density waves or to spatio-temporal chaotic dynamics. We find that the formation of spatially ordered density is favoured by narrow channels and dissipative granular media whereas chaotic dynamics appears for large channels and weakly dissipative grains.

This paper is organized as follows. In Section 2, starting from the kinetic theory model of Jenkins and Savage, we derive equations of motion for quasi-one-dimensional flows through vertical channels. In Section 3, we investigate the linear stability of the steady homogeneous flow whereas Section 4 is devoted to the nonlinear analysis of the flow dynamics. Finally, the summary together with outlooks are presented in Section 5.

[a] e-mail: valance@truffaut.uni-rennes1.fr
[b] UMR 6626.

2 Theoretical approach

Our approach is based on the Jenkins-Savage model inspired by the kinetic theory of gases. First, we will write down, in the framework of the kinetic theory, the general equations of motion for a granular gas flowing in a vertical channel and will determine the properties of a steady homogeneous two-dimensional flow. Then, on the basis of these results we will derive a simplified version of equations of motion for quasi-one-dimensional systems.

We consider a granular gas, composed of identical rigid spherical particles of diameter σ whose collisions are characterised by a fixed coefficient of restitution e, flowing through a vertical channel under gravity. The fields of interest will be the mass density ρ (or equivalently the packing fraction ν), the mean velocity $\mathbf{v}$ about which the actual particle fluctuates and the granular temperature T (that measures the energy per unit mass of the velocity fluctuations). According to the Jenkins-Savage model [3], the equation of motions for a granular gas are given

$$\frac{\partial \rho}{\partial t} = -\boldsymbol{\nabla} .(\rho \mathbf{v}) \,, \tag{1}$$

$$\rho \frac{D\mathbf{v}}{Dt} = \rho \mathbf{g} + \boldsymbol{\nabla} .P \,, \tag{2}$$

$$\frac{3}{2}\rho \frac{DT}{Dt} = -\boldsymbol{\nabla} .\mathbf{Q} + \mathrm{tr}(PE) - \gamma \,, \tag{3}$$

where D/Dt is the material derivative, P the stress tensor, $\mathbf{Q}$ the heat flux, E the symmetrized velocity gradient tensor and γ represents the rate of energy loss due to inelastic collisions. These three equations are nothing but the balance laws for mass, linear momentum and energy fluctuations. We should point out that the interaction between the grains and the surrounding air is neglected here. This is justified as soon as the grain diameter is large enough so that the drag force due to air is small compared with the gravity force. In the case of a flow composed of steel beads moving at an average speed of 1 m/s, the drag force can be safely neglected if the bead diameter is of order of millimetre or larger.

These equations of motion which are of quite general nature must be supplemented by constitutive relations. Here we employ the constitutive relation derived by Jenkins and Savage using a kinetic approach [3]. The stress tensor assumes the standard hydrodynamic form

$$P = -p_h I + 2\eta (E - \frac{1}{3}\boldsymbol{\nabla}.\mathbf{v}\, I) \,, \tag{4}$$

where I is the unit tensor, p_h the pressure and η the viscosity. In the limit of dense granular gases, the pressure and the viscosity are given by

$$p_h = 4\rho G T \,, \tag{5}$$

$$\eta = b\sigma\rho G T^{1/2} \,, \tag{6}$$

with

$$G \equiv \nu g_0(\nu) = \frac{\nu(2-\nu)}{2(1-\nu)^3} \,. \tag{7}$$

$b \simeq 2/\pi^{1/2}$ and g_0 is the radial distribution function [12] which depends on the solid volume fraction ν ($\nu = \rho/\rho_s$ where ρ_s is the particle mass density). We recall that σ is the particle diameter. The heat flux and the dissipation are given by

$$\mathbf{Q} = -\kappa \boldsymbol{\nabla} T = -c\sigma\rho G T^{1/2} \boldsymbol{\nabla} T \,, \tag{8}$$

$$\gamma = d(\rho/\sigma)(1-e) G T^{3/2} \,. \tag{9}$$

κ is the heat conductivity and the quantities c and d are numerical constants ($c \simeq 24/\pi^{1/2}$ and $d = 24/\pi^{1/2}$).

To complete the description, the equations of motion (1–3) should be supplemented by the boundary conditions at the channel walls. Theses conditions are nothing but the balance of collisional exchange of momentum and energy expressed at the channel walls. Here we will consider the walls to be rigid planes to which particles of the same nature to those of the flow are attached. The bumpiness of the walls will be characterised by an angle θ that measures the average depth that a flow particle can penetrate between wall particles.

We are now in position to determine the properties of steady homogeneous flows through vertical channels. We will restrict our analysis to narrow channels where the shear zone is expected to span the full width of the flow. (Ox) will be referred to as the axis perpendicular to the flow direction (the origin O is chosen to be at the middle of the channel) and (Oz) as the axis parallel to the flow. The system is invariant in the (Oy) direction. For steady homogeneous flows, the equations of motion (2–3) reduce to

$$p_h = 4\rho G T^2 = constant \,, \tag{10}$$

$$S = b\sigma\rho G T^{1/2} \partial_x u = -g \int_0^x \rho(\xi) d\xi \,, \tag{11}$$

$$\partial_{xx} T^{1/2} - k^2 T^{1/2} = 0 \,, \tag{12}$$

where S is the shear stress, u is the component of the velocity field along the z coordinate, and $k^2 = (1/bc\sigma^2)[bd(1-e) - 4S^2/p_h^2]$.

In order to pursue our analytical treatment, we will introduce some simplifications. We will consider that the density ρ and the temperature T are practically constant over the flow width. Although these assumptions are not fully consistent with equation (12), we will see that the physical coherence of the problem is still preserved. Taking advantage of these two assumptions, we get

$$S = -\rho g x \,, \tag{13}$$

$$u(x) = u^* - g\frac{[x^2 - (l/2)^2]}{2b\sigma G T^{1/2}} \,, \tag{14}$$

where u^* is the slip velocity at the walls and l is the channel width.

The slip velocity is determined thanks to the balance of momentum at the walls which yields [13]

$$u^* = (\pi/2)^{1/2} f\, T^{1/2} S^*/p_h \,, \tag{15}$$

where S^* is the shear stress at the walls and f is the slip coefficient. f depends only on the walls bumpiness and for small values of the bumpiness angle θ, $f \simeq 2/\theta^2$. The temperature of the flow is determined by the balance of energy at the walls which requires that the dissipation D due to collisions between the particles of the flow and the walls equals the rate of working of the shear stress through the slip velocity. Consequently, we have

$$D = u^* S^* \,, \tag{16}$$

where D is given by [13]

$$D = (2/\pi)^{1/2} h \, (1-e) T^{1/2} p_h \,. \tag{17}$$

The coefficient h depends only on the bumpiness ($h \simeq 1 + \theta^2/4$). Combining the boundary conditions (15–16) with equations (10, 13), we obtain the expression for the granular temperature of the flow

$$T = \frac{gl}{8\mu G} \,, \tag{18}$$

with $\mu = [2(1-e)h/\pi f]^{1/2}$.

The properties of the steady homogeneous flow are now completely determined. Taking advantage of the expression for the temperature, one can rewrite the velocity field as

$$u(x) = u^* + \Delta u \, [1 - (2x/l)^2] \,, \tag{19}$$

with

$$u^* = (\pi/2)^{1/2} f \, \left[\frac{\mu g l}{8G(\nu)}\right]^{1/2} \,, \tag{20}$$

$$\Delta u = \frac{l}{b\sigma} \left[\frac{\mu g l}{8G(\nu)}\right]^{1/2} \,. \tag{21}$$

We can indeed note that given the flow density ρ (or equivalently the packing fraction ν), the channel width l and the bumpiness angle θ of the walls, the velocity profile is entirely determined. Moreover, a careful analysis shows that the slip velocity u^* is a decreasing function of the wall bumpiness angle whereas Δu (which characterizes the shear rate at the walls) increases with the wall roughness. Finally, one should point out that such a parabolic velocity profile has been measured recently by the Clément's Group [14] for particles flowing in a vertical narrow pipe. For large pipes, the measured profile deviates however significantly from the parabolic profile, but this is not surprising since our development is expected to be valid only for narrow channels.

Before proceeding further, we shall introduce an additional quantity (which will be needed later on), that is the mean flow velocity U over the width of the channel. The calculation for U yields

$$U = u^* + \frac{2}{3}\Delta u = \left(1 + \frac{2}{3\lambda}\right) u^* \,, \tag{22}$$

where

$$\lambda = (\pi/2)^{1/2} b(\sigma/l) f \sim (\sigma/l)/\theta^2 \,. \tag{23}$$

In the limit of small bumpiness angles (*i.e.*, $\theta < (\sigma/l)^{1/2}$), λ is greater than unity so that $U \simeq u^*$ (the mean flow is then mainly controlled by the slip velocity). If we restrict our analysis to bumpiness angles $\theta < 0.25$, the approximation is legitimate as soon as the channel width is less then 50σ, which is consistent with the fact that our approach is expected to be valid only for flows through narrow channels. In this limit, all the physical quantities can be expressed as a function of the mean velocity U in a simple manner. Indeed, the granular temperature, the viscosity, the pressure and the shear stress at the walls can be rewritten as

$$T^{1/2} = (2/\pi)^{1/2} \frac{U}{\mu f} \,, \tag{24}$$

$$\eta = (2/\pi)^{1/2} b\sigma\rho G \frac{U}{\mu f} \,, \tag{25}$$

$$p_h = (8/\pi)\rho G \frac{U^2}{\mu^2 f^2} \,, \tag{26}$$

$$S^* = \mu \, p_h \,. \tag{27}$$

These results are not surprising and are consistent with those found for a granular material under shear stresses [3]. In addition we should point out here that the shear stress at the walls is proportional to the square of the mean velocity U which is itself proportional to the shear rate $\Delta u/l$ (see Eq. (21)) and thus follows Bagnold's law [15].

The last step of our strategy is to use the properties of the steady homogeneous flow to write down a simplified version of the equations of motion for quasi-one-dimensional systems. Quasi-one-dimensional systems refer to flows which can be simply described by their mean density and velocity over the channel width. We shall consider here only flow regimes which deviates slightly from the steady homogeneous flow and assume again that the flow density (or packing fraction) remains practically constant over the channel width. For such flow regimes we reasonably expect that the local properties (temperature, pressure and viscosity) of the flow depend only on the local mean velocity U and the packing fraction ν, and that they obey the expressions found in the steady homogeneous flow regime (Eqs. (24–26)). As a consequence, the temperature, the pressure and the viscosity are only dependent of the spatial coordinate z through the variation of the local mean velocity $U(z)$ and packing fraction $\nu(z)$. For such flow regimes, the equation for the local mean velocity U is obtained by considering the balance equation for momentum (Eq. (2)) projected onto the flow direction and integrated along the transverse direction

$$\rho \left(\frac{\partial U}{\partial t} + U \frac{\partial U}{\partial z}\right) = \rho g - \frac{\partial}{\partial z}\left(p_h + \frac{4}{3}\eta \frac{\partial U}{\partial z}\right) - \frac{2S^*}{l} \,. \tag{28}$$

Taking advantage of the expressions of η, p_h and S^* (Eqs. (25–27)), the equation for U finally reads

$$\nu l\left(\frac{\partial U}{\partial t}+U\frac{\partial U}{\partial z}\right)=\nu g l-\alpha(\nu)U^2 - l\frac{\partial}{\partial z}\left[\beta(\nu)U^2\right]-\frac{l^2}{3}\frac{\partial}{\partial z}\left[\gamma(\nu)\frac{\partial U^2}{\partial z}\right] \quad (29)$$

with $\alpha(\nu)=[16/\pi\mu f^2]\nu G(\nu)$, $\beta(\nu)=[1/2\mu]\alpha(\nu)$, $\gamma(\nu)=[\lambda/2]\alpha(\nu)$. The right side of this equation embraces four factors affecting the granular flow. The second term represents the shear stress due to the walls of the channel. The third one is a moderating term due the pressure gradient and the last term models the viscosity effect of the granular gas. Combining equation (29) with mass conservation equation

$$\frac{\partial \nu}{\partial t}+\frac{\partial(\nu U)}{\partial z}=0\,, \quad (30)$$

we have a close set of equations for the mean velocity U and the packing fraction ν. This set of equations is reminiscent of those proposed in traffic flow models [16]. The stationary solution of these equations corresponds to the steady homogeneous flow. It is characterized by a mean velocity U_0

$$U_0=\left[\frac{\nu_0 g l}{\alpha(\nu_0)}\right]^{1/2}=(\pi/2)^{1/2}f\,\left[\frac{\mu g l}{8G(\nu_0)}\right]^{1/2}\,, \quad (31)$$

for a packing fraction ν_0.

3 Linear analysis

The natural next step is to study the linear stability of the steady homogeneous flow. The principle consists in analysing fluctuations about the uniform steady solution by linearizing the motion equations (29–30) with respect to the amplitude of these fluctuations. For that purpose, we assume that the packing fraction and the velocity of the homogeneous flow undergo a small perturbation:

$$\nu=\nu_0+\epsilon\nu_1 e^{iqz+\Omega t}\,, \quad (32)$$

$$U=U_0+\epsilon U_1 e^{iqz+\Omega t}\,. \quad (33)$$

ϵ is a small parameter, q is the wave number of the perturbation and Ω is its growth rate. Plugged into the motion equations (29, 30), we get to first order in ϵ

$$\Omega=ikU_0-\frac{g}{U_0}\left(1+i\frac{\beta_0}{\alpha_0}ql+\frac{\gamma_0}{3\alpha_0}q^2l^2\right) +\frac{g}{U_0}\left[\left(1+i\frac{\beta_0}{\alpha_0}ql+\frac{\gamma_0}{3\alpha_0}q^2l^2\right)^2 -\frac{U_0^2}{g}\left(1-\alpha_0'\frac{U_0^2}{gl}\right)iq-\frac{\nu_0\beta_0'}{\alpha_0}\frac{U_0^2}{gl}q^2l^2\right]^{1/2} \quad (34)$$

where we have set $\alpha_0=\alpha(\nu_0)$, $\beta_0=\beta(\nu_0)$, $\gamma_0=\gamma(\nu_0)$ and the primes stand for derivatives with respect to ν. For small wave numbers, we can perform an expansion in power of q. For the real part of the growth rate, we get

$$\Re(\Omega)=B(\nu_0)q^2l^2-C(\nu_0)q^4l^4+o(q^5)\,, \quad (35)$$

where

$$B(\nu_0)=\left[\frac{U_0^2}{4gl}(1-\alpha_0'\frac{U_0^2}{gl})^2-\frac{\beta_0}{\alpha_0}\right]\frac{U_0}{l}\,. \quad (36)$$

The coefficient C depends on the packing fraction ν_0 and is found to be always positive. The stability of the flow is determined by the sign of the real part of the growth rate. The flow is stable if $\Re(\Omega)<0$ for all q modes. Conversely, it is unstable if there exist at least one wave number for which $\Re(\Omega)>0$.

Let us make first general comments before computing equation (35).

(i) For long wavelength deformation, the term proportional to q^2 in (35) is dominant and then will determine the stability of the steady homogeneous flow. The sign of this term is given by that of the coefficient B which consists of two contributions (see expression (36)). The first contribution is positive and thus plays a destabilising role. It expresses the competition between the gravity force f_g and the shear force S^* (due to the channel walls) as a result of density fluctuations: $\delta f_g\sim g\delta\nu$ and $\delta S^*\sim\alpha_0'U_0^2\delta\nu$. In general, the resulting force is non-zero and tends to destabilize the steady homogeneous flow. In the present situation, the shear force always dominates over the gravity force. The second contribution in B is negative and plays therefore a stabilizing role. It expresses the effect of the pressure gradient which tends to reduce the flow inhomogeneities. Depending on the strength of the stabilising contribution and of the destabilising one, the steady homogeneous flow will be either stable or unstable.

(ii) The second term in (35) (which is proportional to q^4) is of smaller order and is thus only pertinent for shorter wavelength perturbations. This term is negative (since the coefficient C is positive) and stands for the stabilising effect of the viscosity which prevents the flow from density fluctuations with arbitrarily small wavelengths.

The computation of equation (35) yields further results. We find that there exists a critical packing fraction ν_c (to be determined below) above which the steady homogeneous flow is stable. All the modes of the perturbation have a negative growth rate (see Fig. 1). On the contrary, below this critical packing fraction the flow destabilizes: there is a band of unstable modes which grow in course time (see Fig. 1). The critical packing fraction ν_c is determined by $B(\nu_c)=0$ which gives

$$\frac{\nu_c^2}{G(\nu_c)}\left[\frac{G'(\nu_c)}{G(\nu_c)}\right]^2=\frac{32}{\pi f^2\mu^2}\simeq\frac{8\theta^2}{(1-e)}\,. \quad (37)$$

The value of ν_c crucially depends on the wall bumpiness and on the dissipative property of the granular media (through the restitution coefficient e), but it is independent of the channel width. In Figure 2, we have plotted ν_c

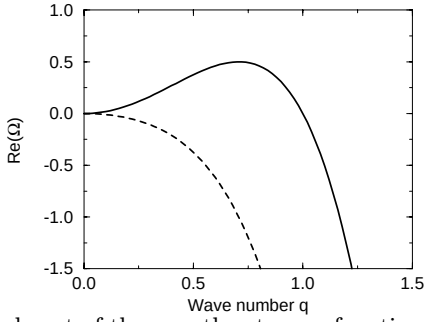

Fig. 1. Real part of the growth rate as a function of the wave number of the perturbation. Full line: unstable. Dashed line: stable.

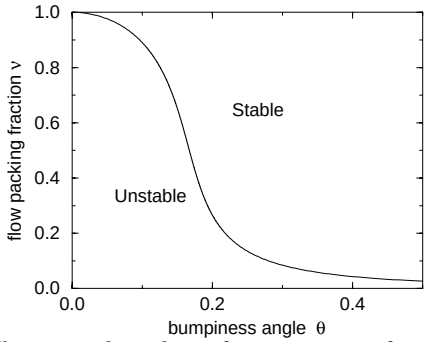

Fig. 2. The critical packing fraction ν_c as function of the bumpiness angle θ. This curve delimits the the region (in parameter space) where the steady homogeneous flow is stable and that where it is unstable.

as a function of the bumpiness angle θ. We can note that ν_c is very sensitive to the wall bumpiness and increases as the wall roughness (*i.e.*, the bumpiness angle) gets smaller. For $e = 0.95$, we find that $\nu_c = 0.5$ for $\theta \simeq 0.17$. For bumpiness angles $\theta < 0.14$, ν_c is found to be greater than the maximum packing fraction of a disordered packing of spheres (*i.e.*, 0.64). This simply means that for these bumpiness angles the steady homogeneous flow can never be stable.

It can be interesting to evaluate the wavelength of the most dangerous mode q_{max} (that is the fastest growing mode). Indeed, the most dangerous mode is expected to prevail in the subsequent nonlinear evolution of the flow and may give an estimate of the wavelength of the spatial ordering of the density waves. Let us first rewrite the real part of the growth rate in the vicinity of the instability threshold. We get

$$\Re(\Omega) \simeq (\nu_c - \nu_0)|B_c'|q^2 l^2 - C_c q^4 l^4 \,, \tag{38}$$

where

$$B_c' \equiv \frac{\partial B}{\partial \nu}|_{\nu=\nu_c} \,, \tag{39}$$

$$C_c \equiv C(\nu_c) = \frac{\lambda}{24}\left(\frac{\nu_c \beta_c'}{\alpha_c} + \frac{\beta_c}{\alpha_c}\right)\frac{U_c}{l}. \tag{40}$$

Note that B_c' is negative. The most dangerous mode q_{max} is then easily calculated

$$l^2 q_{max}^2 = \frac{|B_c'|}{2C_c}(\nu_c - \nu_0) \,. \tag{41}$$

For rather high packing fraction (*i.e.*, $\nu_c > 0.5$), we find that the wavelength Λ_{max} of the most dangerous mode ($\Lambda_{max} = 2\pi/q_{max}$) scales approximatively as

$$\Lambda_{max}/l \sim \theta\,(\sigma/l)^{1/2}(\nu_c - \nu_0)^{-1/2} \,. \tag{42}$$

It should be noted that the wavelength Λ_{max} of the most dangerous mode does not scale linearly with the channel width l but as the square root of l. In addition, we expect that Λ_{max} increases as the bumpiness angle decreases. For $(\nu_c - \nu_0) \sim 0.1$, $\theta \sim 0.2$ and $l \sim 10\sigma$, Λ_{max} is found to be of order of five time the channel width.

To complete this stability analysis, we should examine the imaginary part of the growth rate. The expansion of equation (34) in power of q gives for the imaginary part of Ω

$$\Im(\Omega) = -U_0\left\{1 + \frac{1}{2}(1 - \alpha_0'\frac{U_0^2}{gl})\right\} q + D(\nu_0)q^3 + o(q^4) \,, \tag{43}$$

where D is a function of the packing fraction that we do not need to specify for the moment. The existence of a non-zero imaginary part entails that the modes of the perturbation are not stationary but are drifting along the flow. The drift velocity V_0 is simply given by $V_0 = -\Im(\Omega)/q$. It yields to lowest order in q

$$V_0 = U_0 + \frac{U_0}{2}\left(1 - \alpha_0'\frac{U_0^2}{gl}\right) = U_0(1 - \nu_0 G_0'/2G_0) \,. \tag{44}$$

It is interesting to note that the drift velocity of the modes of the perturbation is always less than the velocity of the flow. Close to the threshold of the instability (*i.e.*, $\nu_0 = \nu_c$), the drift velocity of the unstable modes is given by $V_c = U_c(1 - \nu_c G_c'/2G_c)$ and is found to be negative. This means that the unstable modes propagate upwards. Furthermore for rather high packing fraction (*i.e.*, $\nu_c > 0.5$), V_c is found to behave as

$$|V_c| \sim \theta\,(1 - e)^{-1/2} \,. \tag{45}$$

V_c therefore increases as the bumpiness angle and the restitution coefficient get larger.

The results of the linear stability analysis suggest that in the unstable regime (close to the instability threshold) the flow should give rise to spatially ordered density waves propagating at the speed V_c. In addition, the order of magnitude of the wavelength characterizing the spatial ordering is expected to be given by that of the most dangerous mode q_{max}. However, only a nonlinear analysis can bring sound informations about the flow dynamics in the unstable regime. The following section is precisely devoted to the subsequent nonlinear evolution of the flow.

4 Nonlinear analysis

In order to investigate carefully the subsequent development of the instability, the nonlinear terms neglected

in the linear analysis should be taken into account. To do this, we shall derive a nonlinear equation for the packing fraction and velocity of the flow by means of a multi-scale analysis. We introduce a small parameter $\varepsilon = (\nu_c - \nu_0)$ which measures the distance from the instability threshold. In Fourier space, we have obtained $\Omega \sim \varepsilon q^2 - q^4 + iq^3$ (*cf.* Eqs. (38, 43)). The imaginary term linear in q has been absorbed by means of Galilean transformation $z \to z - V_0 t$. As seen in the previous section, the fastest growing mode corresponds to a wave number which scales as $\sqrt{\varepsilon}$ and the corresponding growth rate scales as ε^2. The imaginary part of Ω would scale as $\varepsilon^{3/2}$ and it dominates in principle. This means that in a multi-scale analysis we have to introduce a short time associated with the propagation and a long time that determines the time scale of the amplification or attenuation of the instability. The total time is $T = T_1 + T_2$ where $T_1 = \varepsilon^{3/2} t$ is the short time and $T_2 = \varepsilon^2 t$ the long time. We will also introduce a slow spatial variable $Z = \sqrt{\varepsilon} z$. The first nonlinear term that appears in the nonlinear expansion of the packing fraction (as well as the flow velocity) is of the form $\nu\nu_z$ and the next one $\nu\nu_{zz} + \nu_z^2$. Both terms scale as ν^2. However the first term contains only one derivative and it is this one which dominates in the long wavelength regime we are interested in. We can show that using a balance between the linear terms and nonlinear ones, the amplitude scales as $\nu \sim \varepsilon^{3/2}$. The strategy is therefore to expand the packing fraction and the velocity of the flow as follows

$$U = U_0 + \varepsilon^{3/2} U_1 + \varepsilon^2 U_2 + \varepsilon^{5/2} U_3 + \dots , \quad (46)$$

$$\nu = \nu_0 + \varepsilon^{3/2} \nu_1 + \varepsilon^2 \nu_2 + \varepsilon^{5/2} \nu_3 + \dots \quad (47)$$

The scheme is to use the motion equations (29, 30) to deduce successively high-order contributions in power of ε. The first non-trivial contribution comes to order ε^3

$$v_1 = -a_0 \nu_1 , \quad (48)$$

$$\frac{\partial \nu_1}{\partial T_1} - a_1 \frac{\partial^3 \nu_1}{\partial Y^3} = 0 , \quad (49)$$

where

$$a_0 = (G_c'/2G_c) U_c , \quad (50)$$

$$a_1 = D_c = \frac{\lambda}{24} (\nu_c G_c'/G_c) l^2 U_c . \quad (51)$$

We recall that D is the coefficient of the cubic term appearing in the imaginary part of the growth rate calculated in Section 3 and that $D_c \equiv D(\nu_c)$. To next order, we get

$$v_2 = -a_0 \nu_2 , \quad (52)$$

$$\frac{\partial \nu_1}{\partial T_2} + \frac{\partial \nu_2}{\partial T_1} = a_1 \frac{\partial^3 \nu_2}{\partial Z^3} - a_2 \frac{\partial^2 \nu_1}{\partial Z^2} - a_4 \frac{\partial^4 \nu_1}{\partial Z^4} + a_3 \frac{\partial \nu_1^2}{\partial Z} , \quad (53)$$

where

$$a_2 = l^2 |B_c'| , \quad (54)$$

$$a_3 = \frac{U_c}{8G_c} \left[2(\nu_c G_c'' + 2G_c') - 3\nu_c \frac{G_c'^2}{G_c} \right] , \quad (55)$$

$$a_4 = l^4 C_c . \quad (56)$$

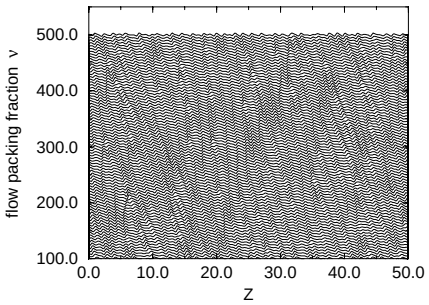

Fig. 3. Spatio-temporal potrait of the packing fraction of the flow for $A_1 = 0.3$.

B_c' and C_c are the coefficients of the quadratic and quartic terms appearing in the real part of growth rate calculated in Section 3 (see Eqs. (39, 40)). Combining equations (49, 53) and setting $\hat{\nu} = \nu_1 + \varepsilon^{1/2} \nu_2$ we obtain

$$\frac{\partial \hat{\nu}}{\partial T} = \varepsilon^{-1/2} a_1 \frac{\partial^3 \hat{\nu}}{\partial Z^3} - a_2 \frac{\partial^2 \hat{\nu}}{\partial Z^2} - a_4 \frac{\partial^4 \hat{\nu}}{\partial Z^4} + a_3 \frac{\partial \hat{\nu}^2}{\partial Z} . \quad (57)$$

Let us make a few comments about this equation. (i) Seeking perturbations of the form $\nu \sim e^{iqZ + \Omega T}$, we recover the linear spectrum $\Omega = a_2 q^2 - a_4 q^4 + i\varepsilon^{-1/2} a_3 q^3$ found in the linear stability analysis. (ii) In absence of the dissipative term this equation reduces the Bürger equation which is variant of the Kuramoto-Sivashinsky equation (KS). When the destabilising term $\hat{\nu}_{zz}$ together with the smoothing one $\hat{\nu}_{zzzz}$ is absent, the equation reduces to the Korteweg-de-Vries equation (KDV). Thus equation (57) is a mixture of the KS equation and KDV equation. KS is known to produce spatio-temporal chaos, while the KDV one gives rise to solitons. The same kind of equation has been already encountered in other physical processes as step-flow growth [17].

In order to analyse the equation (57), we find it convenient to rescale all the variables in a such that only one parameter survives. Making the transformation $\hat{\nu} \to (a_2/a_3)(a_2/a_4)^{1/2} \hat{\nu}$, $T \to (a_4/a_2^2) T$ and $Z \to (a_4/a_2)^{1/2} Z$, equation (57) reads

$$\frac{\partial \hat{\nu}}{\partial T} = A_1 \frac{\partial^3 \hat{\nu}}{\partial Z^3} - \frac{\partial^2 \hat{\nu}}{\partial Z^2} - \frac{\partial^4 \hat{\nu}}{\partial Z^4} + \frac{\partial \hat{\nu}^2}{\partial Z} \quad (58)$$

where $A_1 = a_1 \varepsilon^{-1/2} / (a_2 a_4)^{1/2}$. It should be noted that in the rescaled variables, the linear spectrum is $\Omega = q^2 - q^4 + iA_1 q^3$. The competition between solitons and chaos depends crucially on the order of magnitude of A_1. This aspect has been already investigated in [17] and we find it worthwhile to recall the main outcomes. For small value of A_1 (see Fig. 3, $A_1 = 0.3$), spatio-temporal chaos prevails. There is no intrinsic order: density waves arise and die in a erratic way. Up on an increase of A_1 there is formation of more pronounced density waves with a tendency towards a spatial ordering. Figure 4 shows the pattern for $A_1 = 2$. Furthermore it is interesting to note that starting from a completely disordered state obtained with $A_1 = 0$ and switching A_1 to 1, one can observe the birth of localised pulse (corresponding to a local increase of the packing fraction) which propagates sideways. The successive passage of the solitons on the initially disordered

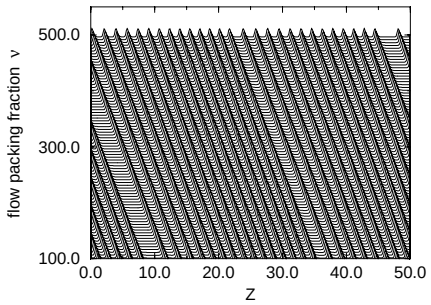

Fig. 4. Spatio-temporal potrait of the packing fraction of the flow for $A_1 = 2$.

pattern leave behind it a more ordered structure. The solitons act as a kind of wavelength selector. However the exact mechanism of selection of the wavelength remains an open question. We can just argue that the wavelength of the pattern is of order of that of the most dangerous mode q_{max} (which is given in the rescaled variables by $q_{max} = 1/2$).

In the light of the above results, it is important to evaluate carefully the order of magnitude of the coefficient A_1 in order to decide which type of structure would be expected in real situations. This coefficient expresses the dispersion of the density waves, indicating that the phase velocity is different from the group velocity. The definition of A_1 entails that this coefficient is rather large since it scales as $\varepsilon^{-1/2}$. This means that close to the onset of the instability dynamics is expected to be regular and to be chaotic as we get away from the instability threshold. In order to be more specific, we need to estimate A_1. Using the expressions of a_1, a_2 and a_4, we find

$$A_1 \sim \varepsilon^{-1/2}\lambda^{1/2}\mu \sim \varepsilon^{-1/2}(1-e)^{1/2}(\sigma/l)^{1/2}. \qquad (59)$$

A_1 is practically independent of the bumpiness angle but it is sensitive to the channel width and to the dissipative properties of the flow particles. A_1 increases as the dissipation increases and as the channel width gets smaller. For $(1-e) \sim 0.1$ and $l \sim 10\sigma$, $A_1 \sim 0.1\ \varepsilon^{-1/2}$. For such parameters, dynamics is regular only very close to the threshold instability (for $\varepsilon \sim 0.01$, $A_1 \sim 1$) and becomes erratic further from the threshold (for $\varepsilon \sim 0.1$, $A_1 \sim 0.3$). For larger channel width ($l \sim 40\sigma$), chaotic dynamics is expected even relatively close to the onset of the instability (since for $\varepsilon \sim 0.01$, $A_1 \sim 0.5$). In addition, our analysis suggests that the more dissipative the granular media is, the more pronounced and ordered the density waves are. These features seem to corroborate recent experimental results obtained for granular flows through vertical channels with serrated walls [18]. These experiments are carried out with particles of large diameter (of order of a few millimetres) varying the channel width and the dissipative properties of the grains and the first outcomes tend to show that the apparition of spatially ordered density waves is favoured by narrow channels and dissipative grains.

5 Conclusion

In summary, we have shown that kinetic model for granular flows can account for the apparition of the density waves resulting from a dynamical instability. Starting from the continuum model of Jenkins and Savage, we have derived equations of motions for flows through narrow channels. The analysis of the motion equations shows that the homogeneous flows destabilises below a critical density in favour of the appearance of density waves. Furthermore the flow dynamics close to instability threshold is expected to be described by an equation which is a mixture between the KS and the KDV equation. The competition between chaos and solitons may lead either to regular spatially ordered density waves or to spatio-temporal chaotic dynamics. We argue that for narrow channels and very dissipative grains, the density waves should be rather regular and exhibit a spatial ordering, whereas for larger channels and less dissipative grains we expect erratic dynamics. We are however aware that our approach suffers from approximations which are not always properly controlled and it would be crucial to confront our predictions with experiments. Our findings are expected to be pertinent for granular flows where the drag force due to air is negligible in comparison with the gravity, namely for flows composed of particles of large diameter (typically of order of millimetre for steel beads). Unfortunately, experiments on granular flows are often carried out with particles of small diameter (between 0.05 to 0.2 mm). To our knowledge, the only experiment using grains of large diameter (of order of a few millimetres) is that of Clément *et al.* [18] and their preliminary results seem to corroborate qualitatively our findings about the nonlinear dynamics of the density waves. The final outcomes of their experiment should bring us valuable informations in order to test quantitatively our overall results.

References

1. D. Bideau, A. Hansen, *Disorder and Granular Media* (North-Holland, Amsterdam, 1993).
2. A. Metha, *Granular Matter: An Interdiciplinary Approach* (Springer Verlag, Heidelberg, 1994).
3. J.T. Jenkins, S.B. Savage, J. Fluid Mech. **130**, 187 (1982).
4. S.B. Savage, J. Fluid Mech. **92**, 53 (1979).
5. T. Pöschel, J. Phys. I France **4**, 499 (1994).
6. S.B. Savage, J. Fluid Mech. **241**, 102 (1992).
7. J. Lee, Phys. Rev. E **49**, 281 (1994).
8. I. Goldhirsch, G. Zanetti, Phys. Rev. lett. **70**, 1619 (1993).
9. F.X. Riguidel, M. Ammi, D. Bideau, A. Hansen, J.C Messager, Powders and Grains, 337 (1993).
10. C. Laroche, S. Douady, S. Fauve, J. Phys. I France **50**, 699 (1989).
11. E. Clément, J. Duran, J. Rajchenbach, Phys. Rev. lett. **69**, 1189 (1992).
12. N.F. Carnahan, K. Starling, J. Chem. Phys. **51**, 635 (1969).
13. J.T. Jenkins, Appl. Mech. Rev. **47**, S240 (1994).
14. E. Clément, G. Reydellet, F. Rioual, in preparation (1998).
15. R.A. Bagnold, Proc. R. Soc. Lond A **255**, 49 (1954).
16. D.A. Kurtze, D.C. Hong, Phys. Rev. E **52**, 218 (1995).
17. C. Misbah, O. Pierre-Louis, Phys. Rev. E **53**, R4318 (1996).
18. F. Rioual, E. Clément, G. Reydellet (private communication).